Intrinsic Mobility Limit for Anisotropic Electron Transport in Alq_3

A. J. Drew,[1] F. L. Pratt,[2] J. Hoppler,[1] L. Schulz,[1] V. Malik-Kumar,[1] N. A. Morley,[3] P. Desai,[4] P. Shakya,[4] T. Kreouzis,[4] W. P. Gillin,[4] K. W. Kim,[1] A. Dubroka,[1] and R. Scheuermann[5]

[1]*Département de Physique, Université de Fribourg, Ch. Du Musée 3, CH-1700 Fribourg, Switzerland*
[2]*ISIS Facility, Rutherford Appleton Laboratory, Chilton, Didcot, Oxon, United Kingdom*
[3]*Dept. of Engineering Materials, University of Sheffield, Sheffield, S1 3JD, United Kingdom*
[4]*Dept. of Physics, Queen Mary, University of London, Mile End Road, London, E1 4NS, United Kingdom*
[5]*Paul Scherrer Institut, PSI-Villigen, Switzerland*

(Received 20 December 2007; published 17 March 2008)

Muon spin relaxation has been used to probe the charge carrier motion in the molecular conductor Alq_3 (tris[8-hydroxy-quinoline] aluminum). At 290 K, the magnetic field dependence of the muon spin relaxation corresponds to that expected for highly anisotropic intermolecular electron hopping. Intermolecular mobility in the fast hopping direction has been found to be 0.23 ± 0.03 cm^2 V^{-1} s^{-1} in the absence of an electric- field gradient, increasing to 0.32 ± 0.06 cm^2 V^{-1} s^{-1} in an electric field gradient of 1 MV m^{-1}. These intrinsic mobility values provide an estimate of the upper limit for mobility achievable in bulk material.

DOI: 10.1103/PhysRevLett.100.116601 PACS numbers: 72.20.Ee, 72.20.Jv, 72.80.Le, 76.75.+i

Electronic devices based on organic semiconductors such as Alq_3 (Fig. 1) have revolutionized electroluminescent displays and large-area electronics [1–5], as they are economically favorable, can be easily processed in large areas, have tunable electronic properties, and are simple to grow into high quality thin films. Even though the mechanisms of charge transport in such organic conductors are fundamental to their operation, many aspects of organic charge transport are still only poorly understood, and progress in this area may be pivotal to utilizing these materials to their fullest extent.

Several types of measurement have been applied to determine carrier transport properties in organic materials. Techniques such as time-of-flight (TOF) and transport-electroluminescence (TEL) can be useful for comparing properties of thin film device materials prepared under varying conditions. However, it is very difficult to extract intrinsic transport properties from such bulk transport measurements without using large single crystals. A completely different class of techniques makes use of a spin probe to measure spin fluctuations at a probe position due to the motion of charge carriers. The spin probe techniques of electron spin resonance (ESR) and nuclear magnetic resonance (NMR) have been used to study carrier diffusion in anisotropic conductors, including doped conducting polymers [6]. In contrast to ESR and NMR, Muon spin rotation, relaxation, or resonance (μSR) has the unique feature that it can both generate an excitation by chemical reaction with the system and also act as a sensitive probe of the dynamics of this excitation [7]. This is particularly important in organic conductors, where muonium forms readily and rapidly reacts with unsaturated bonds. Thus, μSR spin dynamics is a particularly powerful probe for conductors with very low concentrations of carriers, due to this feature of self-generation of carriers. This contrasts with the other probes of spin dynamics, which are more suited to highly doped materials. As a result of the single-point nature of the spin probe, it is highly sensitive to intrinsic transport properties, even in polycrystalline material. In contrast, macroscopic transport probe measurements are usually dominated by extrinsic properties, such as intergrain hopping.

μSR measurements on Alq_3 are reported here. Pure polycrystalline Alq_3 was obtained in the form of bright yellow needles by the multiple sublimation of 99.995% pure material, which was then pressed into tablets. The μSR sample was a mosaic of these tablets, measuring $15 \times 25 \times 2$ mm, mounted on a 99.99% pure silver holder. In the μSR technique [8–10], the temporal evolution of spin polarized muons implanted in the sample is detected through the muon decay positrons, which are emitted primarily along the spin direction of the muon at time of decay and are detected using an array of scintillation

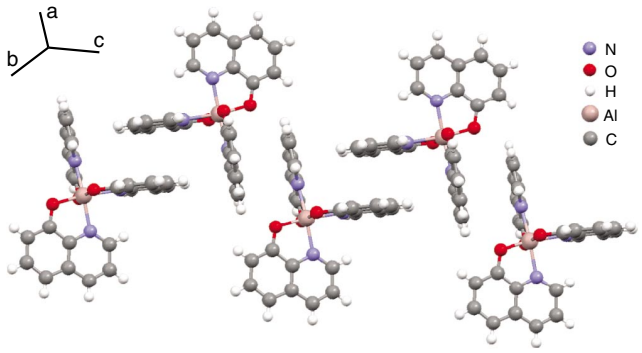

FIG. 1 (color online). The crystal structure of the β phase of Alq_3 [18], showing the good $\pi - \pi$ orbital overlap between ligands of different molecules along the c axis that is responsible for highly one-dimensional motion of charge carriers.

counters. The main part of the experiment was performed on the EMU spectrometer at the ISIS Facility. A longitudinal geometry was employed in which the magnetic field was applied along the initial direction of the muon spin. Detectors were positioned along the beam direction in front of and behind the sample. Relaxation spectra were determined from the time-dependent positron count rates in the forward $F(t)$ and backward $B(t)$ detectors. Each measurement consisted of approximately 20×10^6 muon decay events.

In Alq_3, it is expected that the muon will thermalize quickly, at which point the muon may capture an electron, forming muonium. The muonium rapidly generates radicals, by reacting with the double bonds in the quinoline ligands. A muonated radical arises formally from the addition of muonium to an unsaturated bond. In this case, the spin density is distributed over the molecule, and therefore the hyperfine interaction is reduced from the vacuum muonium case (4463 MHz), often by an order of magnitude or more [11]. Following rapid electronic and structural relaxation of the surrounding molecule, a polaron is formed which is delocalized across the molecule. In a molecular conductor such as Alq_3, the polaron can move away from its initial site and diffuse through the system. As the polaron diffuses, spin flip can occur due to spin-lattice relaxation and interaction with magnetic impurities. This relaxation of the polaron spin will be transferred to the muon via a hyperfine coupling mechanism, but only while the mobile polaron is within interaction range of the muon site. By studying the longitudinal magnetic field (LF) dependence of the muon relaxation, important information about the polaron motion can be obtained [7,12]. In the β phase of Alq_3, molecular overlap occurs in well-defined chain directions along the c axis (see Fig. 1) and the transport in Alq_3 is therefore expected to be dominated by a hopping-type mechanism, not dissimilar to the hopping-type mechanisms responsible for polaron motion in polymeric systems.

In the earlier muon studies of conducting polymers [13–15], spectral density functions from NMR theory were adapted to the muon analysis, resulting in the muon spin relaxation being fitted to an exponential decay function. Risch and Kehr (RK) [16] pointed out that the standard NMR theory used for this data analysis is not strictly valid, as it assumes the existence of a finite correlation time that is short compared to all other time scales in the problem. They considered a more appropriate theory of 1D stochastic charge-carrier motion. The three microscopic parameters in the RK model are the hyperfine coupling ($\omega_0 = 2\pi A$, assumed isotropic), the electron spin relaxation rate (ν, resulting from interaction with spin defects or excitations of the lattice), and the site-to-site hopping rate D. The muon relaxation function is determined by these three parameters plus the time-dependent probability function for the return of the electron to the origin, which contains all the information about the mechanisms and dimensionality of the diffusion. For finite longitudinal fields, the RK model predicts that the depolarization of the muon spin yields a relaxation function of the form [16]

$$G(t) = \exp(\Gamma t)\mathrm{erfc}(\sqrt{\Gamma t}) \tag{1}$$

for $\nu t_{\max} \gg 1$, where erfc is the complimentary error function, $t_{\max}$ the experimental time scale, and Γ the relaxation parameter. Figure 2 shows the measured $F(t) - B(t)$ detector asymmetry taken at a temperature of 290 K, for a wide range of applied magnetic fields, fitted to the RK relaxation function. From the fits shown in Fig. 2, it is clear that the muon spin relaxation is in good agreement with the RK model, confirming the predominantly 1D character of the charge motion. The field dependence of the RK relaxation rate is given by [16]

$$\Gamma = \nu/(1 + 2D\sqrt{2\omega_e\nu}/\omega_0^2)^2 \tag{2}$$

where ω_e is the electron precession frequency, given by $\omega_e/2\pi = \gamma_e B$ where B is the applied magnetic field and the electron gyromagnetic ratio $\gamma_e = 28.024\ \mathrm{GHz\,T^{-1}}$. In the fast diffusion limit, the relaxation parameter effectively becomes independent of ν and inversely proportional to B and the square of the jump rate D

$$\Gamma = \frac{\omega_0^4}{8\omega_e D^2}. \tag{3}$$

Figure 3 shows the magnetic field dependence of the fitted RK relaxation parameter at $T = 290$ K. Fitting the relaxation parameter, Γ (above the decoupling field), to a power law $\Gamma(B) = CB^n$, where C is a constant of propor-

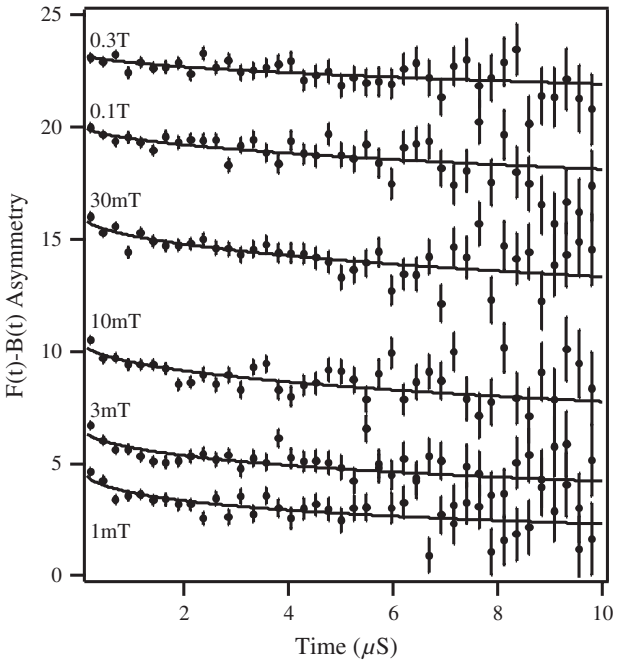

FIG. 2. Positron $F(t) - B(t)$ emission asymmetry for Alq_3 taken at $T = 290$ K for a representative number of longitudinal magnetic fields, showing the muon spin relaxation as a function of time. The solid lines are fits to the RK function (1).

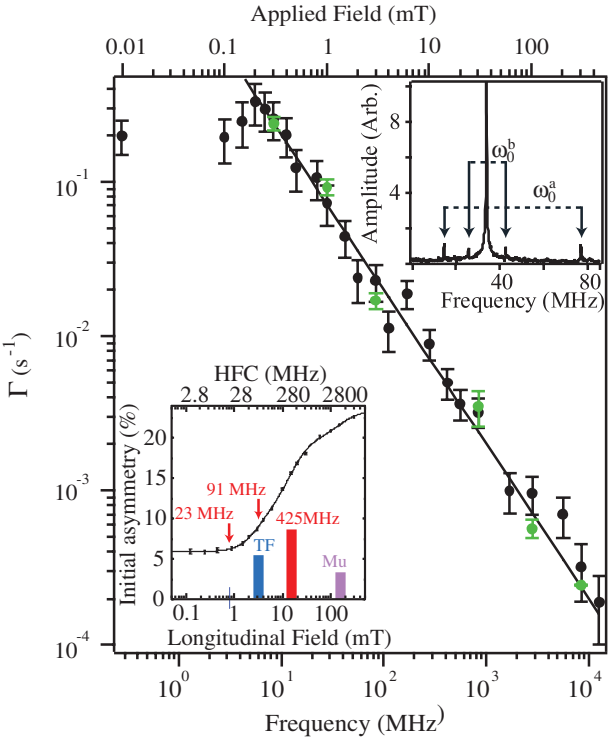

FIG. 3 (color). The muon spin relaxation parameter as a function of applied field, where a B^{-1} dependence is observed, which is characteristic of 1D diffusion in the RK treatment. At longitudinal fields below ~0.2 mT, nearby proton nuclear spins are still coupled to the muon. Black: data taken using fly-past mode. Green: data taken using the high-voltage sample holder at 0 V. Inset (top): A Fourier spectrum in an applied transverse field of 250 mT, which allows us to identify two hyperfine coupling constants a and b (see text). Inset (bottom): The fitted LFQ, showing the three different contributions of the different hyperfine parameters (see text), a contribution from diamagnetic muons (TF) and one from unbound muonium (Mu). The bar heights indicate the weight of each contribution.

tionality, results in an exponent $n = -0.98 \pm 0.03$. This is consistent with the fast hopping limit of the RK model [7], from which charge-carrier hopping rates, and ultimately mobility, can be obtained.

With independent knowledge of the muon hyperfine coupling constant, it is possible to estimate the intermolecular diffusion rate [12,17]. The hyperfine coupling constants can be estimated using a number of methods, including time integral longitudinal field quenching (LFQ) of the asymmetry [12], measuring the Zeeman splitting of the muonium levels in the Paschen-Back [high transverse field (HTF)] limit and via an avoided level crossing (ALC) technique [10], allowing the separation of the isotropic and anisotropic (dipolar) constants. We have performed all three types of measurements on our sample. The HTF measurements were performed in a transverse field of 0.25 T on the GPS instrument at the SμS facility, and two well resolved pairs of radical frequencies were observed, shown in the top-right inset of Fig. 3, corresponding to hyperfine couplings of $\omega_0^a/2\pi = 91 \pm 1$ MHz and $\omega_0^b/2\pi = 23 \pm 1$ MHz. Further confirmation of the radical ω_0^a was obtained using ALC measurements on the Dolly instrument at SμS. However, these two states account for only a minor fraction of the total radical component of the signal, and by analyzing the ISIS LFQ data, we find that a third state c with hyperfine coupling $\omega_0^c = 425 \pm 20$ MHz provides the dominant contribution (see bottom-left inset of Fig. 3).

Fitting the data shown in Fig. 3 to a three component analogue of (3), with each component weighted according to their contributions extracted from the LFQ measurements, yields a hopping rate $D = 1.4 \pm 0.2 \times 10^{12}$ s^{-1}. The intermolecular diffusion constant along the chain is related to the hopping rate by $\mathcal{D} = a^2 D/2$, where a is the site separation. The molecular separation in Alq_3 along the chains shown in Fig. 1 is 0.85 nm [18]. This is also consistent with the intersite hopping distance in amorphous vacuum evaporated films obtained by applying a Brownian motion theory of hopping [19]. Thus, the zero electric-field intermolecular diffusion constant in Alq_3 is obtained to be $\mathcal{D} = 5.1 \pm 0.8 \times 10^{-3}$ cm^2 s^{-1}.

In order to search for a possible change in the electron mobility under an applied electric field, the sample was remounted behind a 50 μm titanium window, clamped between a high-purity aluminum frame and the sample plate. The frame or window and sample plate were insulated with polytetrafluoroethylene to allow high voltages (HV) to be applied to the top of the sample, with the sample plate grounded. A HV of -2 kV was applied to the titanium window, corresponding to an electric-field gradient of 1 MV m^{-1}. As illustrated schematically in the inset of Fig. 4, two routing signals were created, represented by red and green lines. They were used so that it was possible to measure both with and without the applied electric field, allowing the data to be stored in separate histograms. The voltage pulse sequence had a 1:1 mark-space ratio, with acquisition gated to the central 92% of the signal, such that data were vetoed during the rise time of the high-voltage supply. Figure 3 also shows the 0 V data (green points) compared to the original data; it is clear that the two sets agree with each other well. On fitting the 0 V data to (3) (shown in Fig. 4), we find that the zero electric-field intermolecular diffusion constant is $1.1 \pm 0.2 \times 10^{-2}$ cm^2 s^{-1}, which is within the experimental error of the original data. This indicates that the HV sample holder does not appreciably change the muon spin relaxation measurement and that there is no space-charge build up due to the electric field.

The comparison of zero electric field (green) and data in an applied HV of -2 kV (red) is shown in Fig. 4, where there is a clear reduction in the relaxation rate. To investigate whether the observed change in relaxation is due to altering the probability of muonium formation by applying an electric field, we have plotted the muon initial asymmetry in the inset of Fig. 4. It is clear there is no significant

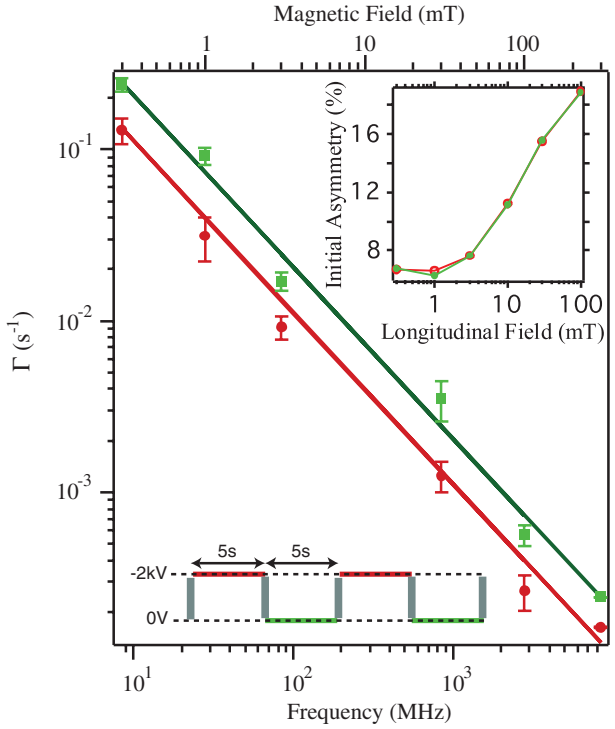

FIG. 4 (color). The muon spin relaxation at 290 K for zero electric field (green) and for an electric field gradient of 1 MV m^{-1} (red). Inset (bottom): schematic diagram of the electric field pulse structure relative to the acquisition electronics (denoted by the line color red: −2 kV; green: 0 V; gray: vetoed). Inset (top): The muon's initial asymmetry, the data taken at −2 kV and 0 V. Errors are approximately the point size.

difference in the initial asymmetry between the two data sets, indicating there is no change in the diamagnetic muon fraction and therefore no change in the muonium formation probability. The decrease in relaxation rate can thus be interpreted as an increase of the intermolecular diffusion constant to $7.9 \pm 1.5 \times 10^{-3}$ cm^2 s^{-1}, resulting from an electric field induced change in the trap distribution.

Applying the Einstein relation to these two diffusion constants, electron mobilities 0.23 ± 0.03 cm^2 V^{-1} s^{-1} and 0.32 ± 0.06 cm^2 V^{-1} s^{-1} are obtained for 0 V and −2 kV, respectively. When compared to the most recent TOF and TEL measurements in Alq_3 (for a summary of recent results, consult Ref. [20]), we find the mobility in zero electric field to be several orders of magnitude larger than the value at the minimum applied field available with these techniques ($\mu \sim 1 \times 10^{-7}$ cm^2 V^{-1} s^{-1} at 5 MV m^{-1}) [20,21]. To put it into context, the mobility of Alq_3 reported here approaches the values observed in 5,6,11,12-tetraphenylnaphthacene (Rubrene) [22]—commonly thought of as one of the best organic semiconductors currently available.

After fitting the cutoff observed in Fig. 3, we are able to extract an upper limit to the "interchain" hopping rate $D_\perp = \gamma_e B_{\text{cut}} = 3.9 \pm 0.9 \times 10^7$ s^{-1}. Assuming four equivalent directions for interchain motion, with an average separation of 0.81 nm [18], gives the interchain diffusion coefficient of $\mathcal{D}_\perp = a^2 D_\perp/4$. The upper limit to the zero field interchain mobility is then $\mu_\perp = 1.2 \pm 0.3 \times 10^{-5}$ cm^2 V^{-1} s^{-1}. For macroscopic TOF/TEL measurements on unoriented films, the observed mobility will be limited to the off-chain value; however, it can often be much smaller due to limitations in the morphology, such as grain boundaries. At the highest reported electric fields, the macroscopic mobilities become comparable with $\mu_\perp$ [20,21], suggesting that grain-boundary resistance is overcome at these fields.

In conclusion, we would like to emphasize that μSR provides an opportunity to measure the intrinsic zero field limit of charge carrier mobilities of organic molecules. The mobilities quoted above represent a ceiling, as the muon measurements are not susceptible to disorder induced bottlenecks present in conventional mobility measurements, especially when considering that our polycrystalline powder samples have an increased crystallinity when compared to the vacuum sublimed films used in the other techniques. The measurements can also be extended to finite electric fields making a reasonable overlap possible with other techniques; however, the RK theory does not include electric-field effects, and some refinement of the RK theory may be required to extract reliable quantitative values under electric-field conditions.

We acknowledge financial support from the Swiss Science Foundation (No. 200021-111690). The μSR experiments were performed at ISIS, Rutherford Appleton Laboratory, UK, and the Swiss Muon Source, Paul Scherrer Institute, Villigen, Switzerland.

[1] H. Sirringhaus *et al.*, Science **280**, 1741 (1998).
[2] M. Granstrom *et al.*, Nature (London) **395**, 257 (1998).
[3] G. Gustafsson *et al.*, Nature (London) **357**, 477 (1992).
[4] R. H. Friend *et al.*, Nature (London) **397**, 121 (1999).
[5] D. Voss, Nature (London) **407**, 442 (2000).
[6] K. Mizoguchi, Jpn. J. Appl. Phys. **34**, 1 (1995).
[7] F. L. Pratt, J. Phys. Condens. Matter **16**, S4779 (2004).
[8] S. J. Blundell, Contemp. Phys. **40**, 175 (1999).
[9] W. Hayes, Phil. Trans. R. Soc. A **350**, 249 (1995).
[10] B. D. Patterson, Rev. Mod. Phys. **60**, 69 (1988).
[11] J. M. Bailey *et al.*, Phys. Rev. A **3**, 871 (1971).
[12] F. L. Pratt *et al.*, Phys. Rev. Lett. **79**, 2855 (1997).
[13] K. Nagamine *et al.*, Phys. Rev. Lett. **53**, 1763 (1984).
[14] K. Ishida *et al.*, Phys. Rev. Lett. **55**, 2009 (1985).
[15] F. L. Pratt *et al.*, Synth. Met. **55**, 677 (1993).
[16] R. Risch and K. W. Kehr, Phys. Rev. B **46**, 5246 (1992).
[17] S. J. Blundell *et al.*, J. Phys. Condens. Matter **14**, 9987 (2002).
[18] M. Brinkman *et al.*, J. Am. Chem. Soc. **122**, 5147 (2000).
[19] L. Ke, J. Appl. Phys. **99**, 114512 (2006).
[20] H. Park *et al.*, Appl. Phys. Lett. **90**, 202103 (2007).
[21] S. Naka *et al.*, Synth. Met. **111**, 331 (2000).
[22] N. Stingelin-Stutzmann *et al.*, Nat. Mater. **4**, 601 (2005).